PAPER

BICM-ID-Based IDMA: Convergence and Rate Region Analyses*

Kun WU[†a)], ***Nonmember***, **Khoirul ANWAR**[†b)], ***and*** **Tad MATSUMOTO**[†,††c)], ***Members***

SUMMARY This paper considers uplink interleave division multiple access (IDMA), of which crucial requirement is the proper operability at a very low signal-to-interference-plus-noise power ratio (SINR) range. The primary objectives of this paper are threefold: (1) to demonstrate the achievability of near-capacity performance of bit interleaved coded modulation with iterative detection (BICM-ID) using *very low rate* single parity check and irregular repetition (SPC-IrR) codes at *a very low* SINR range, and hence the technique is effective in achieving excellent performance when it is applied for IDMA, (2) to propose a very simple multiuser detection (MUD) technique for the SPC-IrR BICM-ID IDMA which does not incur heavy *per-iteration* computational burden, and (3) to analyze the impacts of power allocation on the convergence property of MUD as well as on the rate region, by using the extrinsic information transfer (EXIT) chart. The SPC-IrR code parameters are optimized by using the EXIT-constrained binary switching algorithm (EBSA) at a very low SINR range. Simulation results show that the proposed technique can achieve excellent near-capacity performance with the bit error rate (BER) curves exhibiting very sharp threshold, which significantly influences the convergence property of MUD. Furthermore, this paper presents results of the rate region analysis of multiple access channel (MAC) in the cases of equal and unequal power allocation, as well as of a counterpart technique. The results of the MAC rate region analysis show that our proposed technique outperforms the counterpart technique.

key words: *IDMA, BICM-ID, EXIT, low-rate code, EBSA*

1. Introduction

The superiority of code division multiple access (CDMA) systems, where the entire bandwidth-expansion factor is allocated only for error correction coding by using very low rate code and no spreading is used, is so well known as to be a fundamental concept of communication theory [1]. To make effective use of this theoretical background, a CDMA technique with chip-level interleaving was proposed in [2] (in fact, [2] presents the original idea of interleave division multiple access (IDMA)). The IDMA concept was reformulated and introduced in [3], [4] and [5]. However, designing such low rate and powerful, near-capacity achieving codes that can be decoded without imposing heavy computational complexity, has long been a bottleneck. A quantitative comparison between an *intermediate* solution (which is a combined use of a convolutional code and a low rate repetition code) and conventional CDMA (where error correction coding and spreading are independently performed) is made by [6]. Quite recently, it has been shown in [7] that IDMA with non-Gray (natural) mapping rules achieves better performance than with the Gray mapping, and such tendency is verified by the EXIT analysis. However, the bit error rate (BER) curves with the technique shown in [7] exhibits error-floor.

The primary objectives of this paper are threefold: (1) to demonstrate the achievability of near-capacity performance of bit interleaved coded modulation with iterative detection (BICM-ID) using *very low rate* single parity check and irregular repetition (SPC-IrR) codes. Hence SPC-IrR BICM-ID is effective in achieving excellent performance when applied for IDMA, (2) to propose a very simple multiuser detection (MUD) technique for the proposed SPC-IrR BICM-ID IDMA which does not incur heavy *per-iteration* computational burden, and (3) to analyze the impacts of power allocation on the convergence property and the rate region of the MUD detector, by using the multi-dimensional extrinsic information transfer (EXIT) chart.

Originally, the idea of the SPC-IrR BICM-ID technique is proposed in [8], where extended mapping (EM) is used for modulation to increase the degrees-of-freedom for flexibly changing the demapper's EXIT curve; with EM, *multiple labeling patterns* are mapped to a single constellation point, and the shape of the demapper's EXIT curve changes according to the labeling pattern allocation. To achieve good matching between the demapper and decoder's EXIT curves while keeping the convergence tunnel open until a point near (1.0, 1.0) mutual information (MI) point in the EXIT chart, [8] also introduces doped accumulator (DACC) and modulation mixing (MM) techniques. The labeling patterns and the SPC-IrR code parameters are optimized in a systematic way by using the EXIT-constrained binary switching algorithm (EBSA). With the technique described above, the error-floor of the BER curves can be eliminated (or at least reduced to a value range below $10^{-6} - 10^{-5}$ of BER).

It should be emphasized that detailing the EBSA algorithm and EXIT analysis is not the purpose of this paper. Instead, this paper uses them as tools for achieving good EXIT curve matching and for analyzing the convergence property of the system, respectively. The reason for

Manuscript received November 4, 2013.
Manuscript revised March 28, 2014.

[†]The authors are with School of Information Science, Japan Advanced Institute of Science and Technology (JAIST), Nomi-shi, 923-1292 Japan.

[††]The author is also with Centre for Wireless Communication, University of Oulu, Finland.

*This research has been conducted as a part of the EU FP7 project, RESCUE, No. 619555.

a) E-mail: kunwu@jaist.ac.jp
b) E-mail: anwar-k@jaist.ac.jp
c) E-mail: matumoto@jaist.ac.jp, tadashi.matsumoto@ee.oulu.fi.

DOI: 10.1587/transcom.E97.B.1483

using SPC-IrR is because of the good matching between the decoder and demapper in terms of the shape of their corresponding EXIT curves *in a very low signal-to-interference-plus-noise power ratio (SINR) range* where IDMA systems are required to properly operate.

A very simple MUD technique is proposed in this paper, which does not involve any statistical signal processing, as opposed to [6]. Since the BER curve exhibits very sharp threshold, the proposed MUD technique only performs repeatedly the inner and global iterations to estimate each user's transmitted sequence and to soft-cancel the symbol estimates from the received composite signal, respectively. Hence the computational complexity with the proposed technique is due mainly to the iteration times, which can well be compromised in exchange for a loss in performance by the EBSA algorithm [8]. The convergence property of MUD is analyzed by the multi-dimensional EXIT chart. It should be noted here that in the MUD performance analysis, we assume the simplest case where there are only two users as in [9], and the signals are transmitted over additive white Gaussian noise (AWGN) channel. This is simply because the purpose of the convergence property analysis is to obtain insightful understanding of the algorithm behavior [9].

The most significant contribution of this paper is the impact analysis of unequal power allocation on MUD convergence property, also by using the multi-dimensional EXIT chart. Note again that since we assume only the simplest two-user IDMA in single-path AWGN channel, power allocation is intuitively equivalent in meaning to each user's transmit signal power. It is shown that with unequal power allocation, smaller *total* received signal-to-noise power ratio (SNR) is required to achieve the BER threshold than with the equal power allocation. This result is consistent to [9].

This paper also provides multiple access channel (MAC) rate region analysis for the simplist two-user IDMA system. It is shown that for the fixed identical rate with two users, smaller MAC rate region (or MAC-pentagon) is required with unequal power allocation than with equal power allocation. This result is also consistent to the result of the impact analysis of unequal power allocation on the convergence property described above. It should be noted that the proposed techniques outperforms the counterpart *intermediate* IDMA solution [6] in terms of achievable rate pair relative to the corresponding MAC region.

The rest of this paper is organized as follows: Sect. 2 briefly describes the motivation of using the SPC-IrR code as a class of very low rate, near-capacity performance achieving codes, suitable to BICM-ID-based IDMA with EM. Section 3 describes the single-user detection (SUD) schemes of BICM-ID-based IDMA, and proposes a new, very simple, yet powerful technique for IDMA-MUD. Section 4 shows the results of the EXIT analysis for the BICM-ID-based IDMA-SUD and IDMA-MUD. Section 5 presents BER performances of SUD and MUD. For MUD, we consider equal and unequal power allocation cases. Section 5 also provides results of the rate region analysis in the two-user IDMA MAC scenario assumed in the convergence analysis part. Section 6 concludes this paper with some concluding statements.

2. SPC-IrR Coding and EM Demapping

In this section, we present the motivation of using very low rate SPC-IrR codes for BICM-ID based IDMA with EM from the viewpoint of the *shape* matching of their EXIT curves. In serially concatenated systems such as BICM-ID, whether or not the system can achieve near-capacity performance depends on the matching between the EXIT curves of the inner and outer components. It is well known that EXIT function is a non-decreasing function of *a priori* MI. In the case of BICM-ID, the EXIT curve of the demapper (including the decoder of DACC (DACC^{-1}, as indicated in Fig. 2). For the sake of notational simplicity, the terminology, demapper, indicates demapper-plus-DACC^{-1} through at this paper), which is the inner component, exhibits convex shape, i.e.,

$$\frac{\partial^2 I_E(dem)}{\partial I_A^2(dem)} \geq 0, \qquad 0 \leq I_A(dem) \leq 1.0, \tag{1}$$

where $I_E(dem)$ is the extrinsic MI between the demapper's output log-likelihood ratio (LLR) and the transmitted coded bit, and $I_A(dem)$ is the *a priori* MI of the demapper. The EXIT curve of convolutional codes exhibits concave shape [6], [10] in a region where $I_A(dem)$ is relatively small, i.e.,

$$\frac{\partial^2 I_A(dec)}{\partial I_E^2(dec)} \leq 0, \text{ for relatively small } I_A(dec), \tag{2}$$

where $I_E(dec)$ is the extrinsic MI between the decoder's output LLR and the transmitted coded bit, and $I_A(dec)$ is the *a priori* MI. Note that $I_A(dec) = I_E(dem)$ and $I_A(dem) = I_E(dec)$.

On the contrary, the EXIT curve of the SPC-IrR codes exhibits convex shape, i.e.,

$$\frac{\partial^2 I_A(dec)}{\partial I_E^2(dec)} \geq 0, \qquad 0 \leq I_A(dec) \leq 1.0. \tag{3}$$

According to the area property theorem [10], the area below the decoder's EXIT curve corresponds to the code rates, which requires the decoder's EXIT curve of the very low rate codes to exhibit a *"reverse-L"* shape. Obviously, since (1)–(3) indicate that to keep the convergence tunnel between the demapper and decoder's EXIT curves open until a point very close to the (1.0, 1.0) MI point in the EXIT chart, SPC-IrR is better suited to BICM-ID than convolutional codes. It should be noted here that if SPC is not used, the code used in this paper is equivalent to non-systematic Repeat Accumulate (RA) code without check node encoder after interleaving. The role of SPC is to further *push* the EXIT curve of the decoder to the right side while not making significant change at the left side. Thereby, it is expected that the decoder's EXIT curve exhibits a *"reverse-L"* shape, by which the narrow tunnel opens until a point very close to

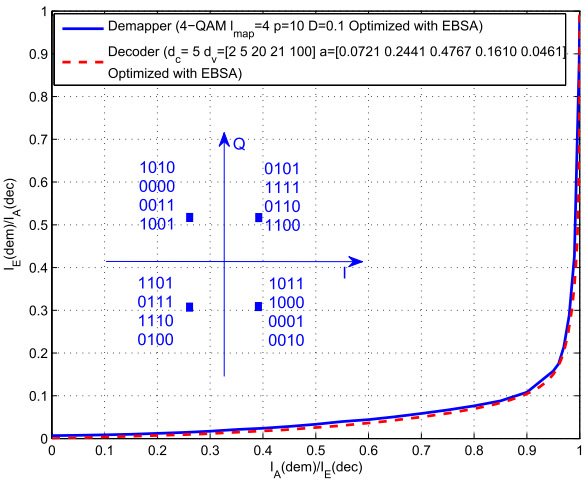

Fig. 1 EXIT chart obtained as the result of EBSA at $SINR = -8.69$ dB (Code rate $R_c = 0.0424$, Spectrum efficiency $\eta_{\text{SPC-IrR}} = 0.1611$ bits/4QAM-symbol).

the (1.0, 1.0) MI point.

In addition, the following three factors provide system design with more degrees-of-freedom: (1) because of the labeling extension with EM, the EXIT curve is further pushed downwards [11], even though the same *physical* constellation is used. The EBSA algorithm [8] can systematically control the trade off between the complexity, represented by the iteraton times and performance loss; (2) regardless of the labelling patterns and SNR values, by using DACC [11], the demapper's EXIT curve reaches a point very close to the (1.0, 1.0) MI point; (3) as described before, MM is also used to flexibly control the shape of the demapper's EXIT curve, where two mapping patterns are mixed at a certain mixing ratio D ($D \times 100\%$ for non-EM and (1-D) $\times 100\%$ for EM, $0 \le D \le 1.0$) [12].

Figure 1 shows the result of labeling pattern optimization for 2-bit extended 4-QAM with its demapper's EXIT curve and the SPC-IrR decoder's EXIT curve; the labeling pattern and the code parameters were jointly optimized for spectrum efficiency $\eta_{\text{SPC-IrR}}$ of 0.1688 bits per 4-QAM symbol (code rate $R_c = 0.0424$) by using EBSA. The parameters related to SPC-IrR, DACC, and MM are presented in the box in the figure.

With EM, l_{map} bits are mapped on to a constellation point in the modulation part. If, 4-QAM, $l_{map} > 2$, more than one labels having different bit patterns are mapped on to each constellation point. D is the parameter that specifies the switching ratio for DACC, where every p-th of the systematic bit is replaced by the accumulated coded bit [11]. SPC code has its parameter d_c, indicating that a single parity bit is added to every $d_c - 1$ information bits. In IrR code, the parameter d_v determines the repetition times for the SPC coded bits, and the ratio is specified by parameter a. Note that IDMA-SUD technique to be described in Sect. 3 will use the same code and labelling parameters as those shown in Fig. 1.

It is found that their EXIT curves are very closely matched, however, the convergence tunnel is open until a point very close to the (1.0, 1.0) MI point. This result has motivated us to design BICM-ID based IDMA using very low-rate SPC-IrR.

3. Detection Schemes

3.1 Single User Detection (SUD)

A schematic diagram of the BICM-ID-based IDMA-SUD is depicted in Fig. 2, where at the receiver the feedback iteration from the demapper output to its input, referred to as global iteration, is not activated. Each user uses the same BICM-ID transmission structure, where the binary bit information sequence $b_{k,i}$ of user-k, $k \in \{1, \cdots, K\}$, at the timing index i is SPC-IrR-encoded at the transmitter. The encoded bit sequence is bit-interleaved by a random interleaver Π_k, and then accumulated by DACC with the switching ratio p to generate a new bits sequence $u_{k,j}$, where j is the timing index at the output of DACC. The DACC output binary sequence $u_{k,j}$ are serial-to-parallel converted, and mapped on to a 4-QAM signal point, in part, according to the labeling pattern depicted in Fig. 1, and in part, according to the non-Gray labeling pattern to produce transmission symbols $x_{k,m}$ at the timing index m, with modulation mixing ratio D.

At the receiver, the received signal r_m at the timing index m can be expressed as

$$r_m = \sum_{k=1}^{K} \sqrt{P_k} \cdot x_{k,m} + n_m, \tag{4}$$

where P_k and n_m denote the power allocated to the k-th user and the AWGN[†] component with variance σ_n^2, respectively. Each user's phase rotation is ignored in (4). This is only because of the simplicity, and in fact, as shown in Appendix for $K = 2$ which is the worst scenario, the two-user's case, one is the case where the phase rotations are ignored, and the other is the case with the phase rotation, yield negligibly minor difference in demapper's EXIT curve. When concentrating on the k-th user, the composite interference composed of the other users' signals is equivalent to noise, and hence, (4) can be rewritten as

$$r_m = \sqrt{P_k} \cdot x_{k,m} + \zeta_{k,m} \tag{5}$$

with

$$\zeta_{k,m} = \sum_{g=1, g\neq k}^{K} \sqrt{P_g} \cdot x_{g,m} + n_m, \tag{6}$$

where $\zeta_{k,m}$ indicates the multiple access interference (MAI) from the other users plus AWGN. It is assumed that $\zeta_{k,m}$ in (5) can be approximated as a Gaussian random variable. Thus, the variance of interference plus noise, experienced by the k-th user, $\sigma^2_{k,\zeta,m}$, at the timing index m, is expressed

[†]As stated in Introduction, since this paper assumes single-path AWGN channel only, power allocation is intuitively equivalent in meaning to each user's transmit signal power.

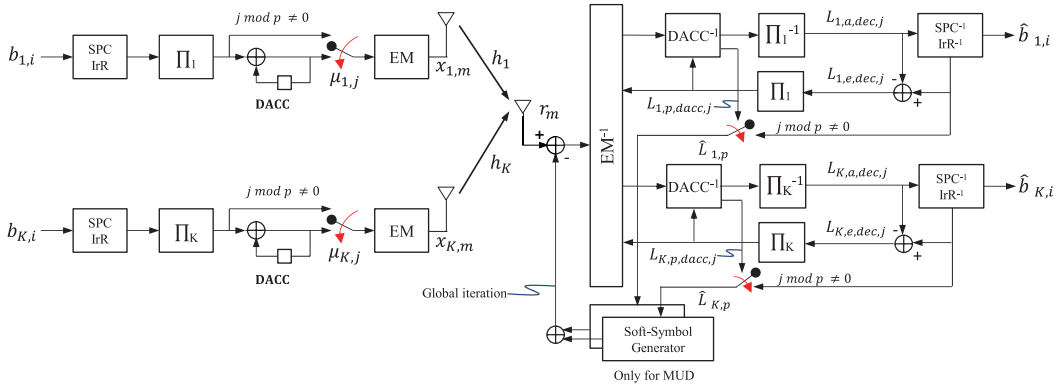

Fig. 2 System model of the proposed BICM-ID-based IDMA systems.

as

$$\sigma^2_{k,\zeta,m} = \sum_{g=1,g\neq k}^{K} P_g + \sigma^2_n, \tag{7}$$

where we assume $\mathbb{E}[|x_{g,m}|^2] = 1$.

The extrinsic information exchange between demapper and decoder is performed iteratively, at the receiver side, adhering the turbo principle. The extrinsic LLR $L_{k,e,dem}$ of the demapper output of the d-th bit in labeling vector corresponding to the transmitted symbol can be expressed as

$$L_{k,e,dem}[b_{k,d}] = \ln \frac{\sum_{x_{k,m}\in S_0} e^{-\frac{|r_m - x_{k,m}|^2}{\sigma^2_{k,\zeta,m}}} \prod_{q=1,q\neq d}^{\ell} e^{-b_q(s)L_{k,a,dem}(b_q(s))}}{\sum_{x_{k,m}\in S_1} e^{-\frac{|r_m - x_{k,m}|^2}{\sigma^2_{k,\zeta,m}}} \prod_{q=1,q\neq d}^{\ell} e^{-b_q(s)L_{k,a,dem}(b_q(s))}}, \tag{8}$$

where $S_0(S_1)$ and $L_{k,a,dem}(b_q(s))$ denote the labelling set, of which the d-th bit is 0(1), and the *a priori* LLR, fed back from the decoder, corresponding to the q-th position in the label allocated to the signal point s, respectively. $L_{k,a,dem}$ is equivalent to extrinsic LLR $L_{k,e,dec}$ of the decoder forwarded via the deinterleaver. q indicates the position of the bits allocated in the symbol $x_{k,m}$. The structure of the decoder as well as mathematical expressions for the decoder's extrinsic LLR calculation can be found in [8].

3.2 Multiple User Detection (MUD)

The global iteration shown in Fig. 2 is now included in MUD. The received signal is expressed by (4)–(6), in the same way as in SUD. However, since the interference from the other users are eliminated by performing soft successive interference cancellation (SSIC) at the receiver side, the mean and the variance of the soft symbol, $\mathbb{E}[|x_{k,m}|]$ and $\sigma^2_{k,x,m}$, respectively, are updated every time the soft symbol is subtracted from the received composite signal, as shown in (16) and (17). The global iteration is activated when no relevant gain in MI is achieved after several inner iterations alone.

The mean and the variance of the k-th user's soft symbol at the timing index m are updated by using

$$\mathbb{E}[|\hat{x}_{k,m}|] = \sum_{x_{k,m}\in S} x_{k,m} \prod_{\varpi=1}^{\ell} P(b_{k,\varpi} = \mp 1), \tag{9}$$

$$\sigma^2_{k,x,m} = 1 - \mathbb{E}[|\hat{x}_{k,m}|]^2 \tag{10}$$

with

$$P(b_{k,\varpi} = W) = \frac{e^{-b_{k,\varpi}\hat{L}_{k,p}}}{1 + e^{-\hat{L}_{k,p}}}, \tag{11}$$

where $W \in \{0, 1\}$ and ϖ is bit index of EM label. S is a set of constellation points. $\hat{L}_{k,p}$ denotes the *a posteriori* LLR fed back via the global iteration to generate the soft symbol replica, $\hat{x}_{k,m} \equiv \mathbb{E}[|x_{k,m}|]$, defined as

$$\hat{L}_{k,p} = L_{k,a,dec,j} + L_{k,e,dec,j} + L_{k,p,dacc,j} \tag{12}$$

Obviously, before the first global iteration is activated, the mean and the variance are initialized, respectively, as

$$\mathbb{E}[|\hat{x}_{k,m}|] = 0, \tag{13}$$

$$\sigma^2_{k,x,m} = 1. \tag{14}$$

The soft interference cancellation can be expressed as

$$\hat{r}^t_m = r_m - \mathbb{E}[|\zeta^t_{k,m}|], \tag{15}$$

where

$$\mathbb{E}[|\zeta^t_{k,m}|] = \sum_{g=1}^{K} \sqrt{P_g} \cdot \mathbb{E}[|x^{t-1}_{g,m}|] - \sqrt{P_k} \cdot \mathbb{E}[|x^{t-1}_{k,m}|]. \tag{16}$$

and t is the global iteration index for each m-th transmission block. Then, the variance of the equivalent noise experienced by the k-th user after the soft cancellation via the global iteration is given by

$$\hat{\sigma}^{t\ 2}_{k,\zeta,m} = \sum_{g=1,g\neq k}^{K} P_g \cdot \sigma^{t-1\ 2}_{g,x,m} + \sigma^2_n. \tag{17}$$

Thus, the equation for demapping, originally given by (8), can be rewritten for MUD as

$$L_{k,e,dem}[b_{k,d}] = \ln \frac{\sum_{x_{k,m}\in S_0} e^{-\frac{|\hat{r}^t_m - x_{k,m}|^2}{\hat{\sigma}^{t\,2}_{k,\zeta,m}}} \prod_{q=1,q\neq d}^{\ell} e^{-b_q(s)L_{k,a,dem}(b_q(s))}}{\sum_{x_{k,m}\in S_1} e^{-\frac{|\hat{r}^t_m - x_{k,m}|^2}{\hat{\sigma}^{t\,2}_{k,\zeta,m}}} \prod_{q=1,q\neq d}^{\ell} e^{-b_q(s)L_{k,a,dem}(b_q(s))}}, \tag{18}$$

where $\hat{r}^t_m$ and $\hat{\sigma}^t_{k,\zeta,m}$ are updated every time the global iteration is activated, before they are provided to the demapper. The demapping equations in (8) and (18) can be calculated efficiently in the log-domain using the Jacobi algorithm [13], [14].

4. EXIT Analysis of BICM-ID-Based IDMA

This section presents results of EXIT analysis for the proposed system. We exactly follow the established methods [10], [15] when calculating the EXIT curves. SINR and SNR for each user are defined as follows

$$SINR_k = \frac{P_k}{\sum_{g=1,g\neq k}^{K} P_g + \sigma_n^2}, \tag{19}$$

$$SNR_k = \frac{P_k}{\sigma_n^2}, \tag{20}$$

where P_k, and σ_n^2 denote the power allocated to k-th user and AWGN noise variance, respectively.

4.1 EXIT Analysis of IDMA-SUD

Assume that the power allocated to each user is identical, i.e., $P_k = 1.0$. We set $\mathrm{SINR}_k = -8.69\,\mathrm{dB}$ for $k = 1, 2, \ldots, 6$, and hence the SUD EXIT chart is identical to that shown in Fig. 1 for SINR= $-8.69\,\mathrm{dB}$ for BICM-ID. The achieved spectrum efficiency $\eta_{SPC-IrR}$ in this case is 0.1611 bits per 4-QAM symbol (code rate $R_c = 0.0424$). With this very low code rate, because of the area property, the area under the decoder curve is very small, which means that the decoder EXIT curve exhibits a *"reverse-L"* shape, and so is the demapper's EXIT curve. Because they are closely matched, near-capacity performance, very sharp BER threshold and error-floor removal (or reduction to a value range below $10^{-6} - 10^{-5}$ of BER) can be expected even with the designed very low-rate code.

4.2 EXIT Analysis of IDMA-MUD

As stated in Introduction, we assume the simplest two-user (K=2) IDMA MAC scenario to identify the convergence property and to focus on the impact of unequal power allocation. We first draw the demapper's EXIT curve by assuming that all the other users' signals are cancelled and we only consider one user. This assumption is reasonable because as described above, labelling patterns and coding parameters are determined by the EBSA algorithm so that two EXIT curves are very closely matched, and hence very sharp BER threshold can be expected. This means that if the labelling patterns and coding parameters are designed at a specified SNR value, SSIC can gradually but finally completely eliminate the other users' signals, without having to involve any statistical signal processing-based interference cancellation, as opposed to [6]. The EXIT curve obtained by using EBSA is presented in Fig. 3 for $SNR_k = -3.8\,\mathrm{dB}$. Since the simultaneous users provide the LLR feedback to each other, three-dimensional (3D) EXIT curves are presented to visualize the convergence property.

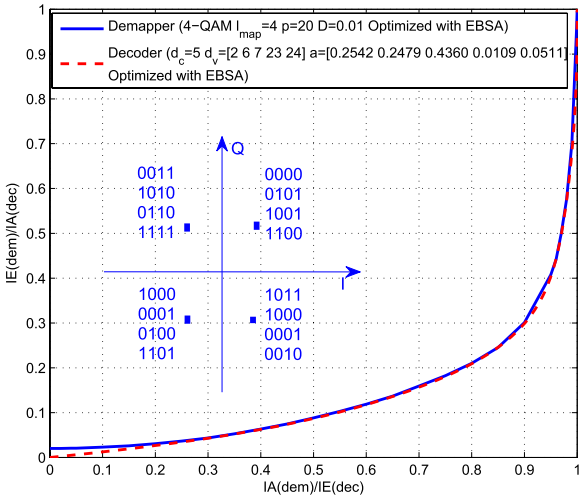

Fig. 3 EXIT chart of IDMA-MUD technique at $SNR_k = -3.8\,\mathrm{dB}$, $k = 1, 2$ (Code rate $R_c = 0.1226$, Spectrum efficiency $\eta_{SPC-IrR} = 0.4879$ bits/4QAM-symbol).

4.2.1 Equal Power Allocation

Assume that the powers allocated to all users are equal which is the same as the power allocation in SUD. A 3D EXIT chart is presented in Fig. 4(a) for $SNR_1 = SNR_2 = -0.8\,\mathrm{dB}$. It is found that the demapper and decoder planes are very close to each other, with a small gap near the (0.0, 0.0, 0.0) MI point. Hence, the LLR exchange can start. The tunnel opens in the most of the areas of the planes, and with the help of SSIC, the gap between the two planes becomes larger, and hence the trajectory is expected to directly reach a point very close to the (1.0, 1.0, 1.0) MI point. This will be confirmed in Sect. 5.2.

4.2.2 Unequal Power Allocation

Assume that the powers allocated to different users are unequal but the total power P_{total} is kept constant. In this paper, $P_{total} = 2.0$, for all the scenarios tested with two-user IDMA-MUD, and the noise variance is changed accordingly in this case. Figure 4(b) presents the 3D EXIT chart in an unequal power allocation scenario where the ratio $P_1/P_2 = 0.68$, $SNR_1 = -3.29\,\mathrm{dB}$ and $SNR_2 = -1.62\,\mathrm{dB}$. It is found that the two planes intersect at the most of the middle part where the decoder's EXIT plane is obviously above the demapper's. However, there still remains a gap, through which the trajectory is expected to go through and reach a

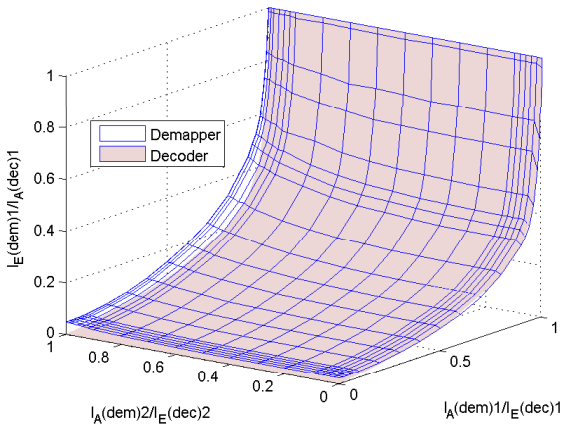

(a) Equal power allocation, $(P_1 + P_2)/\sigma_n^2 = 2.21$ dB.

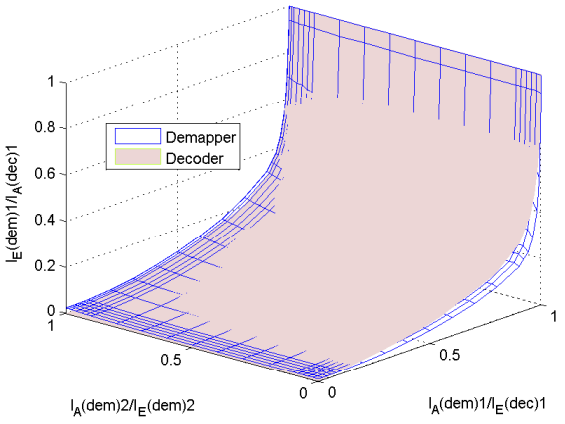

(b) Unequal power allocation, $(P_1 + P_2)/\sigma_n^2 = 0.63$ dB.

Fig. 4 3D EXIT chart of IDMA-MUD technique.

point very close to the (1.0, 1.0, 1.0) MI point. It should be noticed that for the both users, the SNR value is less than −0.8 dB, which is the case of equal power allocation, tested in the previous Sect. 4.2.1. This makes significant impact on the MAC region to be analysed in Sect. 5.3.

5. Performance Evaluation

5.1 Performance of IDMA-SUD

BICM-ID-based IDMA-SUD does not require soft interference cancellation, and it only performs demapping and decoding, user-by-user, independently, without providing any *a priori* information to help the other users. Therefore, for IDMA-SUD, the BER performance versus SINR, defined by (19), is not affected by the number of the users, if the total user number K and the noise variance σ_n^2 are fixed. Figure 5 plots BER performance of the proposed BICM-ID-based IDMA-SUD for $K = 6$, shown by "○". The BER threshold is very sharp, and no error floor can be observed (or invisible within the BER value range shown in the figure). It is found that the threshold SINR is around −8.69 dB, which is exactly consistent with the EXIT chart shown in

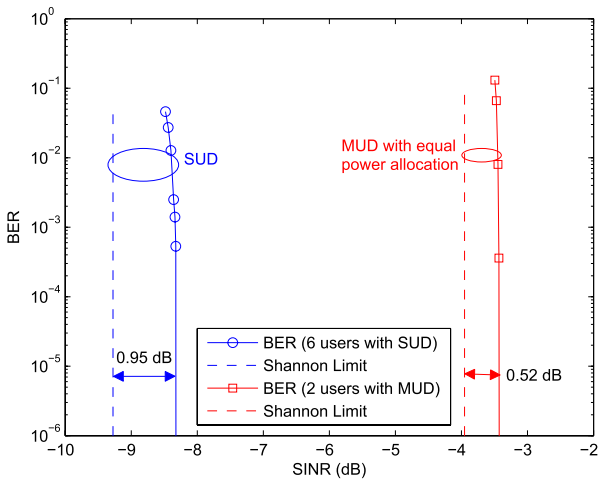

Fig. 5 BER performance of IDMA-SUD and IDMA-MUD with equa power allocation (In MUD case, SINR is defined without SSIC).

Fig. 1, and this observation is independent of the number of the simultaneous users. The consistency between Figs. 1 and 5 indicates that it is reasonable to approximate the composite signal composed of the simultaneous users' signals plus Gaussian noise by equivalent Gaussian noise having the same power, at least, in a low enough SINR range.

5.2 Performance of IDMA-MUD

With the proposed BICM-ID-based IDMA technique, excellent BER performance versus SINR can be achieved with SUD. However, when the number of users increases, BER versus each user's SINR, defined by (19), degrades due to the multiple access interference from the other simultaneous users. Therefore, to achieve better performance, a technique to reduce or to ultimately eliminate the interference, such as SSIC, is needed. Again, the simplest two-user scenario is assumed, and this section investigates the BER performance of *user 1* with the SSIC IDMA-MUD as a reference. The trajectory indicating the MI exchange obtained through chain simulation is also presented.

5.2.1 Performance of Equal Power Allocation

Figure 6 presents 3D EXIT chart and the trajectory of the proposed BICM-ID-based IDMA-MUD for $K = 2$ users, respectively, where the $SINR_1 = SINR_2 = -3.43$ dB ($SNR_1 = SNR_2 = -0.8$ dB and $(P_1 + P_2)/\sigma^2 = 2.21$ dB). The BER performance in this scenario is shown by "□" in Fig. 5. With our proposed technique, the BER threshold is very sharp and no error-floor is visible in the BER range. Due to the exactly matched EXIT curves combined with the soft cancellation technique, very near-capacity performance, only 0.52 dB away from the limit, can be achieved. It is found that the trajectory directly goes through the middle part between the two planes, and reaches a point very close to the (1.0, 1.0, 1.0) MI point, as expected in Sect. 4.2.

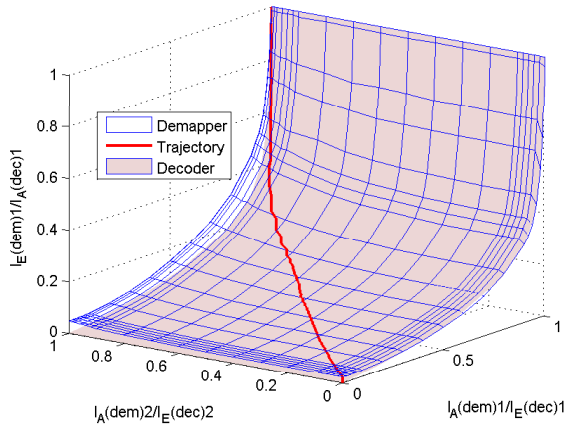

Fig. 6 The trajectory of IDMA-MUD with equal power allocation.

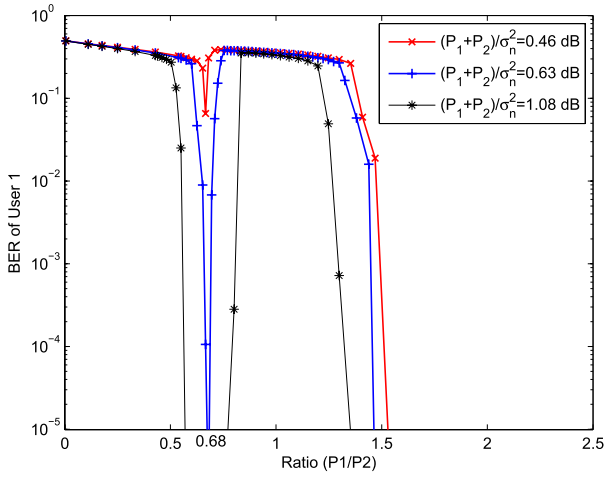

Fig. 7 BER performance of IDMA-MUD for $K = 2$ users with unequal power allocation.

5.2.2 Performance of Unequal Power Allocation

Assume that the total power is fixed as $(P_1 + P_2) = 2.0$ such that $(P_1 + P_2)/\sigma_n^2 = 1.08\,\text{dB}$, while changing the ratio of P_1/P_2. The results of the simulations conducted to evaluate the BER performance with unequal power allocation, are plotted in Fig. 7. It is found from the figure that the BER curve shown by "*" for *user 1* first decreases very sharply as the ratio P_1/P_2 increases, and it becomes lower than 10^{-5} between $P_1/P_2 = 0.58$ and $P_1/P_2 = 0.75$, and then it suddenly increases to a value larger than 10^{-1}, when $P_1/P_2 \cong 1.0$. Then, after that, it sharply decreases again when $P_1/P_2 \geq 1.3$. When the $(P_1 + P_2)/\sigma_n^2$ is decreased to 0.63 dB, the BER curve shown in "+" has almost the same tendency, still the rapid decrease in BER can be found around $P_1/P_2 = 0.68$, when the ratio $P_1/P_2 < 1.0$. However, the BER curve shown in "×" is for $(P_1 + P_2)/\sigma_n^2 = 0.46\,\text{dB}$ where the same labelling pattern and code parameters, including the switching and mixing ratios, p and D, respectively, are used as in the case of $(P_1+P_2)/\sigma_n^2 = 1.08\,\text{dB}$. A similar tendency can be observed but the rapid decrease in BER can not be observed, when the ratio $P_1/P_2 < 1.0$. Hence, $(P_1 + P_2)/\sigma_n^2 = 0.63\,\text{dB}$ is identified as the limit case with this set of code parameters and labelling pattern. In the following part, we focus on the limit case so as to make comparison among several unequal power allocation cases as well as with a counterpart technique, shown in Sect. 5.3.

The trajectories representing the MI exchange are investigated at the ratios of $P_1/P_2 = \{1.0, 0.6, 0.68\}$ with $(P_1 + P_2)/\sigma_n^2 = 0.63\,\text{dB}$. Figure 8(a) shows the trajectory for $P_1/P_2 = 1.0$ in the 3D EXIT chart. It is found that although there is a gap between the planes of demapper and decoder, the trajectory is stuck at a relatively low MI point. This is because with $P_1/P_2 = 1.0$, $SNR_1 = SNR_2 = -2.38\,\text{dB}$ and $(P_1 + P_2)/\sigma_n^2 = 0.63\,\text{dB}$, the two planes are so close to each other around the (0.0, 0.0, 0.0) MI point and hence the trajectory can not go through the tunnel. Figure 8(b) shows the trajectory for $P_1/P_2 = 0.6$ ($SNR_1 = -3.62\,\text{dB}$, $SNR_2 = -1.4\,\text{dB}$ and $(P_1 + P_2)/\sigma_n^2 = 0.63\,\text{dB}$). It is found that the two planes intersect in the most of the middle part of the 3D EXIT chart, however, there still exists a small gap on the left side of the intersected area, and the tunnel is open until the extrinsic MI of the demapper for *user 1* is around 0.35 and hence the trajectory can reach the point (demapper's extrinsic MI = 0.35 for the *user*1). Furthermore, it is found from the trajectory that for *user 2*, decoder's extrinsic MI reaches very close to 1.0. This means that *user 2* can be nearly fully detected without errors while *user 1* can not be fully detected. Figure 8(c) presents the trajectory for $P_1/P_2 = 0.68$ ($SNR_1 = -3.29\,\text{dB}$, $SNR_2 = -1.62\,\text{dB}$ and $(P_1 + P_2)/\sigma_n^2 = 0.63\,\text{dB}$). It is found that the two planes intersect in the most of the middle part of the 3D EXIT chart, but a gap still exists near the left edge of the two planes, and the tunnel opens until a point very close to the (1.0, 1.0, 1.0) MI point. The trajectory can sneak through the gap between the two planes, and reach the point very close to (1.0, 1.0, 1.0) MI point, which also means both the two users can be fully detected, even with smaller $(P_1 + P_2)/\sigma_n^2$ value (0.63 dB), compared with equal power allocation case, whose $(P_1 + P_2)/\sigma_n^2$ value is 2.21 dB.

5.3 MAC Rate Region Analysis

It is of our great interest to make the MAC rate region comparison between equal and unequal power allocation cases, as well as between our proposed and [6]'s proposed technique. The scenario with $K = 2$ is considered for the both equal and unequal power allocation cases. To calculate the MAC rate region, we assume that all the users use Gaussian codebook. The points in the MAC rate region A_1 and A_2, as defined in Fig. 9, are given by

$$A_1 = C\left(\frac{P_1}{\sigma_n^2}\right), \tag{21}$$

$$A_2 = C\left(\frac{P_1}{P_2 + \sigma_n^2}\right), \tag{22}$$

with $C(x) = \log_2(1 + x)$.

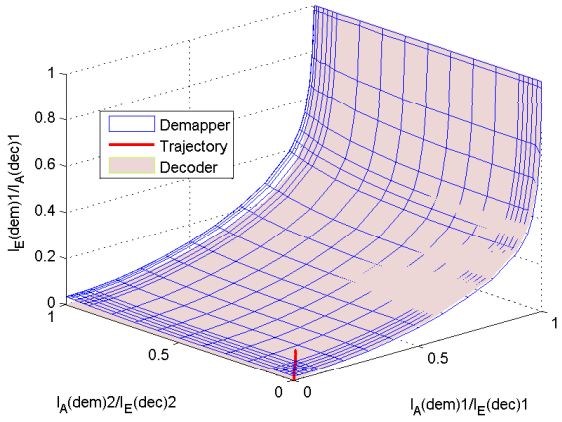

(a) $P_1/P_2 = 1$, $(P_1 + P_2)/\sigma_n^2 = 0.63$ dB.

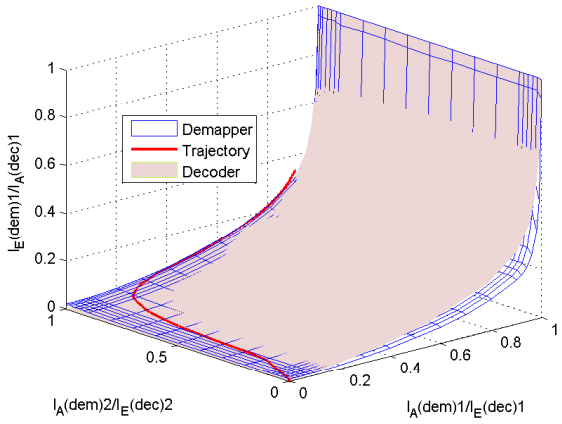

(b) $P_1/P_2 = 0.6$, $(P_1 + P_2)/\sigma_n^2 = 0.63$ dB.

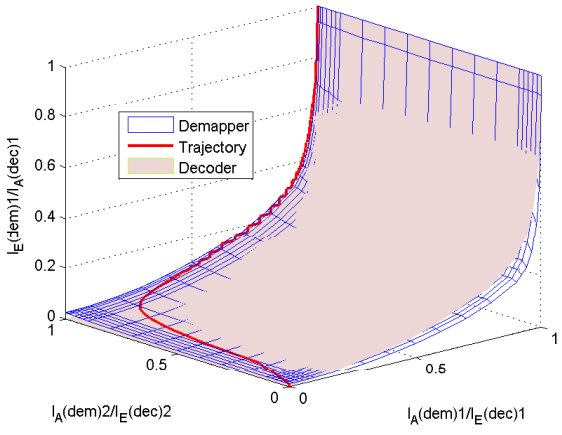

(c) $P_1/P_2 = 0.68$, $(P_1 + P_2)/\sigma_n^2 = 0.63$ dB.

Fig. 8 The trajectories of IDMA-MUD with unequal power allocation.

B_1 and B_2 are defined in the same way as the points A_1 and A_2 by replacing the user index 1 by 2. Moreover, since we are assuming $P_1 = P_2 = 1.0$ for the case of equal power allocation, and $P_1 + P_2 = 2.0$, while changing σ_n^2 and P_1/P_2 values for the unequal power allocation case.

From Fig. 5 we first determined the $SINR_k$ value required to achieve 10^{-6} BER for $P_1/P_2 = 1.0$ and $(P_1 + P_2)/\sigma_n^2 = 2.21$ dB, then, all the values of the argument of $C(x)$, which is needed to calculate (21), (22), can be determined for equal power allocation case. For the unequal power allocation case, those values were directly obtained from $P_1/P_2 = 0.68$, $(P_1 + P_2)/\sigma_n^2 = 0.63$ dB and $P_1 + P_2 = 2.0$ (Recall that the rapid decrease of BER happens at $P_1/P_2 = 0.68$, as shown in Fig. 7). Figure 9 shows the MAC rate regions (or MAC-pentagon) with the equal and unequal power allocation cases. It is found that the MAC rate region with unequal power allocation is smaller than that with equal power allocation. However, the achieved spectrum efficiency of two cases are the same, i.e., $R_1 = R_2 = \eta_{\mathrm{SPC-IrR}} = 0.4879$ bits per 4-QAM symbol, which is shown in Fig. 9 by "○". This confirms that unequal power allocation can achieve the same spectrum efficiency with smaller SNR values of each user.

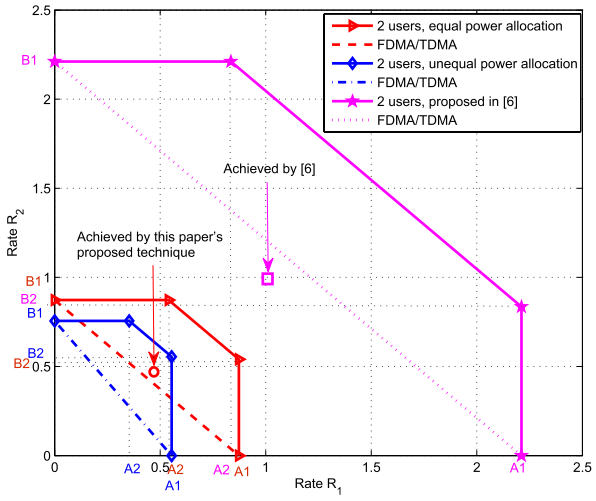

Fig. 9 Gaussian multiple access channels for $K = 2$ users (the comparison between our proposed IDMA (with equal and unequal power allocation cases) and IDMA proposed in [6]).

The dashed line connecting A_i and B_i, $i = \{1, 2\}$, corresponds to two-user orthogonal signalling such as frequency or time division multiple access (FDMA or TDMA). It is found that with both the equal and unequal power allocation cases, the rate-pair plot is above the FDMA/TDMA line, and with the unequal power allocation, the plot is closer to the theoretical MAC rate region.

The upper bound of the sum-rate $R_1 + R_2$ is given by

$$R_1 + R_2 \leq C\left(\frac{P_1 + P_2}{\sigma_n^2}\right) \tag{23}$$

It is found from Fig. 9 that the MAC rate region with unequal power allocation is smaller than that with equal power allocation, and obviously, with the unequal power allocation, the MAC region is not symmetric. With the equal power allocation ($SNR_1 = SNR_2 = -0.8$ dB), the sum-rate bound B_{equal} is 1.41, while with unequal power allocation ($SNR_1 = -3.29$ dB and $SNR_2 = -1.62$ dB), the sum-rate bound $B_{unequal}$ is 1.1. Therefore, we can conclude that the

achieved sum-rate $R_1 + R_2 = 2 \times 0.4879$, and $R_1 + R_2 < B_{unequal}$ ($SNR_1 = -3.29$ dB and $SNR_2 = -1.62$ dB)$< B_{equal}$ ($SNR_1 = SNR_2 = -0.8$ dB). It can be concluded that to achieve the same spectrum efficiency ($\eta_{\mathrm{SPC-IrR}} = 0.4879$), unequal power allocation requires smaller $SNRs$ values for each user.

It is interesting to make comparison of the achieved rate pair and the MAC rate region between our proposed and [6]'s proposed techniques. Since [6] assumes an 8 user IDMA scenario, we converted the rate pair and the MAC region to the two-user case by the following method: first of all, we identified the SNR value, required to achieve 10^{-6} BER from Fig. 3 in [6]. Since, in [6], all users use the same code, which achieves 0.2550 bits per 4-QAM symbol, and the same power is allocated to them, A1 point in Fig. 9 can be calculated by assuming that 6 out of 8 users are totally cancelled, and A2 by assuming that 6 out of 8 users are equivalent to noise. The point B1 and B2 can also be calculated in the same way.

Since spectrum efficiency of the system proposed in [6] is 0.2550 bits per 4-QAM symbol for all the 8 users, it is equivalent to each user's spectrum efficiency of 1.02 bits per 4-QAM symbol in two-user case, assuming a Gaussian codebook. The calculated MAC region and the rate pair (indicated by "□") obtained by converting from 8 user IDMA to two-user IDMA are also shown in Fig. 9. It is found that surprisingly the achieved rate pair with [6]'s technique is lower than the FDMA/TDMA line with a Gaussian codebook. Obviously, this is because the code used in [6] (a convolutional code combined with a low rate repetition code) can achieve neither near-capacity performance nor very sharp BER threshold.

6. Conclusions

In this paper, we have focused on an up-link multiple access technique with IDMA that requires proper operability at very low SINR range. First of all, we have verified the near-capacity performance of BICM-ID using very low rate SPC-IrR codes, designed by an optimization algorithm for BICM-ID, EBSA. Results of simulations, conducted to verify the performance of the proposed technique, were then presented. It has been shown that near-capacity performance, very sharp BER threshold and error floor removal (or at least reduced to a value range below $10^{-6} - 10^{-5}$ of BER) can be achieved at a very low SINR range where IDMA systems are required to properly work. Therefore, the proposed technique is effective in achieving excellent performance when it is applied for IDMA. Motivated by the very sharp BER threshold, a new yet simple MUD technique for IDMA was proposed, which does not require heavy *per-iteration* computational burden. This paper then analyzed the convergence and the MAC rate region properties. Multi-dimensional EXIT chart was used as a tool for the analysis. It has been shown that even though the demapper and decoder's EXIT planes are very closely matched, the trajectory sneaks through the small gap between the planes and reaches a point very close to the (1.0, 1.0, 1.0) MI point. Furthermore, the results of the MAC rate region analysis show that to achieve the same spectrum efficiency, unequal power allocation requires smaller MAC rate region (or MAC-pentagon) compared with the equal power allocation; the proposed IDMA technique outperforms a counterpart technique in terms of the rate pair relative to the MAC region. The results of the performance analyses and evaluations shown in this paper are all consistent with each other.

Acknowledgment

The authors are sincerely grateful for the support provided by KDDI R&D Laboratories Inc. and Hitachi Kokusai Electric Inc. through technical discussions. The authors also acknowledge help of Mr. Soulisak Ormsub, Mr. Meng Cheng, and Mr. Xin He for their helpful discussions.

References

[1] A.J. Viterbi, "Spread spectrum communications-myths and realities," IEEE Commun. Mag., vol.17, no.3, pp.11–18, May 1979.
[2] P. Frenger, P. Orten, and T. Ottosson, "Code-spread CDMA using maximum free distance low-rate convolutional codes," IEEE Trans. Commun., vol.48, no.1, pp.135–144, Jan. 2000.
[3] H. Schoeneich and P.A. Hoeher, "Adaptive interleave-division multiple access — A potential air interference for 4G bearer services and wireless LANs," WOCN, pp.179–182, Muscat, Oman, June 2004.
[4] P.A. Hoeher and H. Schoeneich, "Interleave-division multiple access from a multiuser point of view," 5-th Int. Symp. Turbo Codes Related Topics Connection 6th Int. ITG-Conf. Source Channel Coding, pp.140–144, Germany, April 2006.
[5] P. Li, L. Liu, K. Wu, and W.K. Leung, "Interleave division multiple access," IEEE Trans. Wireless Commun., vol.5, no.4, pp.938–947, April 2006.
[6] K. Kusume, G. Bauch, and W. Utschick, "IDMA vs. CDMA: Detectors, performance and complexity," IEEE Global Telecommunications Conf. (GLOBECOM 2009), pp.1–8, Hawaii, USA, Nov. 2009.
[7] H.H. Chung, Y.C. Tsai, and M.C. Lin, "IDMA using non-Gray labelled modulation," IEEE Trans. Commun., vol.59, no.9, pp.2492–2501, Sept. 2011.
[8] K. Fukawa, S. Ormsub, A. Tolli, K. Anwar, and T. Matsumoto, "EXIT-constrained BICM-ID design using extended mapping," EURASIP J. Wireless Commun. and Networking, vol.2012, no.1, Feb. 2012.
[9] S. Verdu, Multiuser Detection, Cambridge University Press, 1998.
[10] J. Hagenauer, "The EXIT chart — Introduction to extrinsic information transfer in iterative processing," 12th European Signal Processing Conf. (EUSIPCO), pp.1541–1548, Vienna, Austria, Sept. 2004.
[11] K. Anwar and T. Matsumoto, "Very simple BICM-ID using repetition code and extended mapping with doped accumulator," Wireless Pers. Commun., Sept. 2011. doi:10.1007/s11277-011-0397-1.
[12] F. Schreckenbach and G. Bauch, "Irregular signal constellations, mappings and precoder," Information Theory and its Applications (ISITA), pp.10–13, Italy, Oct. 2004.
[13] R. Lidl and H. Niederreiter, Finite Fields, Cambridge University Press, 1996.
[14] S. Lin and D.J. Costello, Error Control Coding, 2nd ed., Prentice Hall, NJ, USA., 2004.
[15] S. ten Brink, "Convergence behaviour of iteratively decoded parallel concatenated codes," IEEE Trans. Commun., vol.49, no.10, pp.1727–1737, Oct. 2001.

Appendix: Gaussian Noise Approximation

It is well-known that when the number of users increases, in multiple access system, the interference from the other users can be approximated as Gaussian noise according to the central limit theorem. However, this paper has assumed instantaneous power control and furthermore the phase rotations have been ignored, which is eventually equivalent to the scenario where all the users transmit the same static AWGN channel. To identify the impact of this assumption on the demapper's extrinsic MI, we evaluate the EXIT curve for $K = 2$, which is the worst scenario, where each user has randomly different phase rotation, resulting in more Gaussian-like receive signal point distribution. The received signal in this case can be expressed as

$$r_m = \sqrt{P_k} \cdot x_{k,m} \cdot e^{j\theta_k} + \zeta_{k,m}, \qquad (\mathrm{A}\cdot 1)$$

where θ_k denotes the phase rotation of k-th user, uniformly distributed over $[0, 2\pi]$. The comparison between the two cases is presented in Fig. A· 1 in terms of the demapper's EXIT curves. It can be observed that the difference in the EXIT curves is negligible.

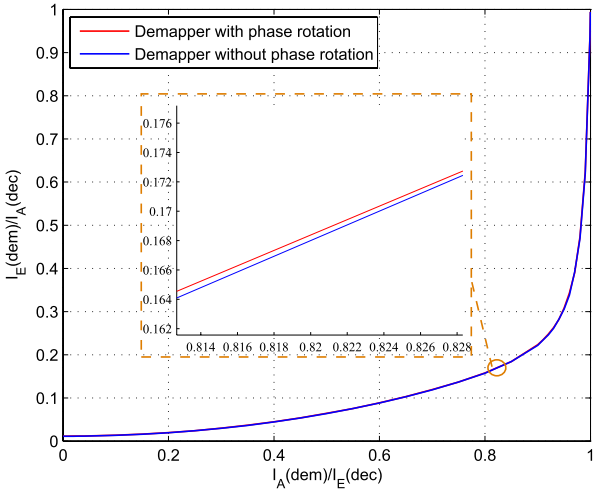

Fig. A· 1 Comparison between the EXIT curves of demapper with and without phase rotations, $K = 2$ users, $SNR = -3.8$ dB.

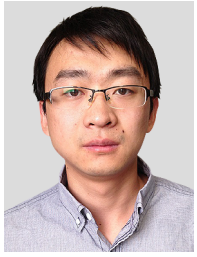

Kun Wu received the B.Sc. in Information and Computing Science from Anhui University of Science and Technology (AHUT), China, in 2010. He is currently perusing his Master degree in the School of Information Science, Japan Advanced Institute of Science and Technology (JAIST), Japan. His research interests are IDMA techniques, code design and system optimization.

Khoirul Anwar graduated (*cum laude*) from the department of Electrical Engineering (Telecommunications), Institut Teknologi Bandung (ITB), Bandung, Indonesia in 2000. He received Master and Doctor Degrees from Graduate School of Information Science, Nara Institute of Science and Technology (NAIST) in 2005 and 2008, respectively. Since then, he has been appointed as an assistant professor in NAIST. He received best student paper award from the IEEE Radio and Wireless Symposium 2006 (RWS'06), California-USA, Best Paper of Indonesian Student Association (ISA 2007), Kyoto, Japan in 2007, and Award for Innovation, Congress of Indonesian Diaspora (CID), Los Angels, USA, July 2012. Since September 2008, he is with the School of Information Science, Japan Advanced Institute of Science and Technology (JAIST) as an assistant professor. His research interests are network information theory, error control coding, iterative decoding and signal processing for wireless communications. Dr. Anwar is a member of IEEE, information theory society, and IEICE Japan.

Tad Matsumoto received his B.S., M.S., and Ph.D. degrees from Keio University, Yokohama, Japan, in 1978, 1980, and 1991, respectively, all in electrical engineering. He joined Nippon Telegraph and Telephone Corporation (NTT) in April 1980. Since he engaged in NTT, he was involved in a lot of research and development projects, all for mobile wireless communications systems. In July 1992, he transferred to NTT DoCoMo, where he researched Code-Division Multiple-Access techniques for Mobile Communication Systems. In April 1994, he transferred to NTT America, where he served as a Senior Technical Advisor of a joint project between NTT and NEXTEL Communications. In March 1996, he returned to NTT DoCoMo, where he served as a Head of the Radio Signal Processing Laboratory. In March 2002, he moved to University of Oulu, Finland, where he served as a Professor at Centre for Wireless Communications. In 2006, he served as a Visiting Professor at Ilmenau University of Technology, Ilmenau, Germany, funded by the German MERCATOR Visiting Professorship Program. In April 2007, he returned to Japan and since then he has been serving as a Professor at Japan Advanced Institute of Science and Technology (JAIST), while also keeping the position at University of Oulu. Prof. Matsumoto has been appointed as a Finland Distinguished Professor for a period from January 2008 thru December 2012, funded by the Finnish National Technology Agency (Tekes) and Finnish Academy, under which he preserves the rights to participate in and apply to European and Finnish national projects. Prof. Matsumoto is a recipient of IEEE VTS Outstanding Service Award (2001), Nokia Foundation Visiting Fellow Scholarship Award (2002), IEEE Japan Council Award for Distinguished Service to the Society (2006), IEEE Vehicular Technology Society James R. Evans Avant Garde Award (2006), and Thuringen State Research Award for Advanced Applied Science (2006), 2007 Best Paper Award of Institute of Electrical, Communication, and Information Engineers (IEICE) of Japan (2008), Telecom System Technology Award by the Telecommunications Advancement Foundation (2009), IEEE Communication Letters Exemplifying Reviewer Award (2011), UK Royal Academy of Engineering Distinguished Visiting Fellow Award (2012) and NiKKei Electronic Wireless Japan Awards (2013). He is serving as an IEEE Vehicular Technology Distinguished Lecturer since July 2011. He is a Fellow of IEEE and a member of IEICE.